Atomic Spectroscopy

Article

Protected Geographical Identification of Honey by Spark Discharge-assisted Laser-induced Breakdown Spectroscopy

Diana Corina Fechner,[a] Tiago Varão Silva,[b] Maurilio Gustavo Nespeca,[b] Alan Lima Vieira,[b] José Anchieta Gomes Neto,[b] Dário Santos Júnior,[c] Roberto Gerardo Pellerano,[a] and Edilene Cristina Ferreira[b,*]

[a] Instituto de Química Básica y Aplicada del Nordeste Argentino (IQUIBA-NEA), UNNE-CONICET, Facultad de Ciencias Exactas y Naturales y Agrimensura, Av. Libertad 5400, 3400 Corrientes, Argentina

[b] São Paulo State University – UNESP, Chemistry Institute of Araraquara, R. Prof. Francisco Degni 55, 14800-900 Araraquara, SP, Brazil

[c] Department of Chemistry, Federal University of São Paulo - UNIFESP, R. São Nicolau 210, 09913-030, Diadema, SP, Brazil

Received: *March 12, 2021;* ***Revised:*** *April 06, 2021;* ***Accepted:*** *April 06, 2021;* ***Available online:*** *April 07, 2021.*

DOI: 10.46770/AS.2021.022

ABSTRACT: Honey is a natural food that is valued worldwide for its nutritional and therapeutic values. Therefore, authentication of honey according to the geographical origin is a guarantee of the genuine properties. In this article, an evaluation of spark discharge-assisted laser-induced breakdown spectroscopy (SD-LIBS) for certification of the geographical origin of honey is reported. Forty-nine samples of multifloral honey produced in four Argentine provinces were considered. The results showed the best classification performance was obtained using smoothing, generalized least squares weighting (GLSW) and mean centering for spectral preprocessing, added to the k-nearest neighbor (k-NN) or Support Vector Machine (SVM) classification algorithms, which provided 100% of correct classification. More importantly, the results of Partial Least Squares – Discriminant Analysis (PLS-DA) pointed to N, Ca, K, Cu, Fe and Mn as key elements for the certification of geographical origin. In addition, the greatest potential of N stands out for the discrimination of the origin of honey. These findings confirm SD-LIBS as a promising tool for authentication of honey quality, providing a simple, fast and environmentally friendly solution. The method can be useful for industry, the market and others related to food authenticity.

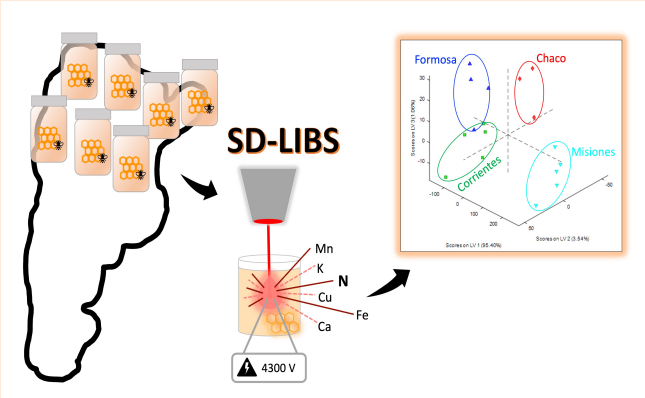

INTRODUCTION

Consumers' lifestyle inquires certificates to prove genuine characteristics of food. Some differentiated foods are labeled by protected geographical identification (PGI) and protected designation of origin (PGO) that requires a premium price for products. Food fraud covers cases where there is a violation of food law, which is intentionally committed to obtain a financial gain through consumer deception.[1]

Honey is the third most adulterated food in the world.[2] Produced by bees from the nectar of plants, honey is a naturally sweet food valued worldwide for its nutritional and therapeutic values[2]. The properties mentioned are intrinsically related to the geographical origin of honey.[3,4] Therefore, authentication of honey according to its origin is an important requirement that demands reliable, fast and reproducible analytical methods.

The method traditionally used to determine botanical and geographical origin of honey is the pollen analysis which reflects the type of vegetation from which the nectar was collected by the bees.[5] The method mentioned is time-consuming and requires great skill and technical experience in pollen morphology.[6] In addition, if honey undergoes a filtration process this type of

analysis becomes infeasible.

In order to simplify the determination of the origin of the honey, methods based on the elemental analysis of the honey composition have been proposed.[7-15] These methods use analytical techniques, such as atomic absorption spectrometry (AAS), inductively coupled plasma optical emission spectroscopy (ICP-OES) and inductively coupled plasma mass spectrometry (ICP-MS) combined with multivariate data analysis. The disadvantages of the aforementioned techniques are the high cost per analysis, since they require gases and high-purity reagents, in addition to the time for the sample pretreatment. Particularly for honey samples, analytical difficulties may arise due to its high carbohydrates content, which influence the performance of the mentioned analytical techniques.[16] Sample pretreatment by wet digestion using concentrated acid and heating[17] or dry ashing followed by ash dissolution in concentrated nitric acid[18] are time-consuming and costly procedures besides not being environmentally friendly. In contrast, the direct analysis of diluted samples using techniques that depend on the nebulization of the sample, such as flame atomic absorption spectrometry (FAAS), ICP-OES and ICP-MS is critically affected by the effects of transport. Considering these disadvantages, direct analysis techniques such as Raman, infrared and some sensors have been explored for classification of honey.[19-22] However, the elemental composition of the samples cannot be accessed by these techniques.

Laser-induced breakdown spectroscopy (LIBS) is an analytical technique capable of performing direct and fast multielement analysis with minimal or no sample preparation, without the use of chemical consumables, such as solvents and gases. LIBS is based on the measurements of atomic and ionic emission of elemental sample constituents excited in a plasma. A single LIBS analysis takes a few seconds to perform. In addition to the elemental analysis, the correlation between spectral fingerprint and other samples properties is also possible.[23,24] Due to its potential, LIBS has been successfully applied to detect food fraud.[25,26] Despite the attractive analytical characteristics, LIBS shows low detectability, which makes some types of application difficult. For this reason, some strategies have been developed to improve the sensitivity of the LIBS, such as the spark discharge-assisted LIBS (SD-LIBS), which increases emission intensities by reheating the plasma.[27]

Recently, Zhao *et al.* (2020)[28] achieved good results for the classification of honey according to geographical origin. The authors used a LIBS system composed by a high-energy laser operating at 532 nm, a high-resolution spectrometer and an intensified detector. In contrast, low-cost LIBS systems have received great attention and expanding the applicability of the technique.[29-30] The low sensitivity and spectral resolution of these instruments have been circumvented using some simple devices to increase sensitivity and applying different spectral processing to extract the appropriate analytical information.[30-32]

In this work, a low-cost LIBS system coupled with a spark-discharge (SD) for authentication of geographical origin of honey was evaluated, taking advantage of the speed and reliability of the LIBS and aiming to provide an accessible device for authentication and traceability of honey.

EXPERIMENTAL

Samples. For this study, forty-nine samples of multifloral honey collected in harvesting season between 2015 and 2016, from four provinces of the Northeast region of Argentina (Fig.1), were used. The extraction and mixing of honey were carried out in an extraction room authorized by the National Service for Agri-food Health and Quality. Each sample corresponded to a composite sample, prepared from the mixture of samples extracted from ten beehives. The use of composite sample was chosen because it provides an unbiased estimation of the population average. Thus, eleven composite samples were obtained from the province of Formosa (F), ten from Chaco (CH), fourteen from Corrientes (C), and fourteen from Misiones (M). The honey samples were stored in polypropylene flasks at room temperature until analysis.

LIBS analysis. The spectra were acquired using a LIBS system designed for direct analysis of solids, which is equipped with a Q-switched laser Nd:YAG 1064 nm Big Sky Ultra 50 (Quantel, Co., Bozeman, MT, USA), an optical fiber bundle, and four spectrometers HR2000+ (Ocean Optics Co., Dunedin, FL, USA), featuring an optical resolution of 0.1 nm (full width at half maximum) and a spectral range from 200 nm to 630 nm. The laser

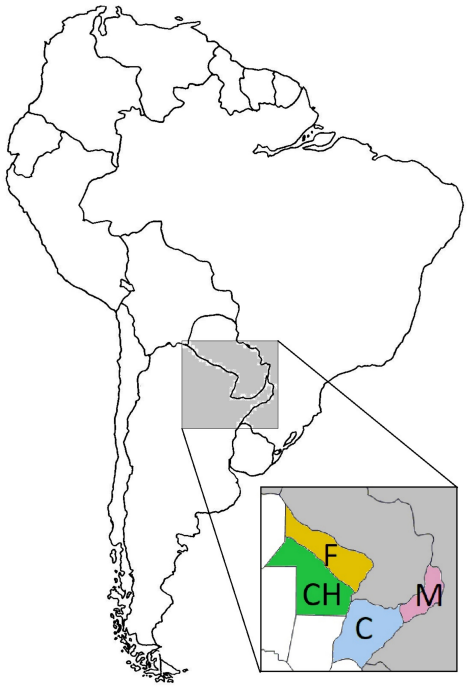

Fig. 1 Geographical location of the Argentine regions producing the studied honey samples.

with pulse duration of 8 ns was operated with a maximum power energy of 50 mJ. The integration time and the Q-Switched delay used for the acquisition of spectra were 1 ms and 2.5 μs, respectively.

The samples were placed in polyethylene sampling flasks until filling out their capacity (around 1 mL). The flask was placed in the sample holder of LIBS system, which can be moved in the x-y directions. The sampling chamber is equipped with video camera to monitor the analyses. A spark discharge device was coupled with LIBS to increase the detectability of emission lines. The spark discharge was obtained using two cylindrical pure tungsten electrodes fixing 4 mm between them and 2 mm above the sample surface. The DC voltage signal was 4300 V. More details on the electric discharge system can be found in Vieira et al. (2018).[33] Twenty spectra were measured for each sample by spreading lasers pulses on the surface of the sample.

Chemometric analysis. All chemometric analysis were performed using MATLAB 2013a (MathWorks Inc., Natick, MA, USA) with PLS toolbox 7.3.1. (Eigenvector Research Inc., WA, USA). The spectral profile of all samples was first evaluated to detect outliers. Spectra showing an anomalous profile, evidenced by the absence of emission signals in any wavelength range, were discarded. Thereafter, each individual spectrum was processed by Whittaker filter for baseline fitting and multiplicative scatter correction (MSC) to normalize the effects of fluctuations, which is common in the LIBS analysis[26,34]. A principal component analysis (PCA) was performed using each preprocessed spectrum. The spectrum that showed scores values beyond the confidence limits (95% level) in the first principal component was excluded. Finally, the spectra corresponding to each sample were averaged. Afterward, the spectrum set was divided into subsets for calibration and validation: two-thirds of the samples were considered for calibration (9 C, 7 CH, 7 F, and 9 M), and one-third for external validation (5 C, 3 CH, 4 F, and 5 M).

Three methods of classification were evaluated, Partial Least Squares Discriminant Analysis (PLS-DA),[35] k-nearest neighbor (k-NN),[36] and Support Vector Machine (SVM).[37] The number of latent variables (LV) used in the PLS-DA model and the number of nearest neighbors (k) were chosen according to the number of correct classifications of the calibration samples during cross-validation. The SVM model was developed using the radial basis kernel type. The values of the SVM parameters (ν and γ) were automatically optimized during cross-validation. The SVMs used for binary classification within a multiclass strategy were based on 0 and 1, with a threshold of 0.5.

The classification methods described were evaluated in combination with the following preprocessing techniques: baseline correction by Whittaker filter, first and second derivatives (15 variables per window), Savitzky-Golay smoothing, MSC by mean, MSC by median, normalization by area, Standard Normal Variate (SNV), Pareto scaling, Poisson scaling, generalized least squares weighting (GLSW), and external parameter orthogonalization (EPO)[38-40]. After the application of each preprocessing, the data were mean centered or autoscaled.

RESULTS AND DISCUSSION

The experimental data were first submitted to the removal of outliers. Thereafter, the remaining spectra were evaluated by PCA, and the scores plot (PC1 *versus* samples) was used as a control chart. Spectra showing scores values out of the confidence limits (95% level) were excluded. The observed outliers may be due to the honey meniscus formed in the sampling flask, which provided different laser focal distance in relation to sample surface, considering the center and the edges of the flask. These differences led to the exclusion of 19% of the spectra. Therefore, the replicates for each sample ranged from 5 to 20. The useful spectra from each sample were adjusted to the baseline, normalized, and averaged.

The classification models were developed using the average spectra of each sample. The first step of the modeling was to determine the most suitable spectral preprocessing for each classification method (PLS-DA, k-NN and SVM). The results of correct classifications for thirteen preprocessing strategies and 30 combinations are shown in Table 1. The mean centering does not influence k-NN and SVM modeling, so this preprocessing was only maintained by convention. Consequently, autoscaling had the same effect as variance scaling using these methods. The combination of smoothing, GLSW, and mean centering provided the highest number of correct classifications for the three methods performed. Since the GLSW attenuates spectral variables that vary in the same class, variables correlated to the classes present greater weight in the modeling. Therefore, this preprocessing was the most important to provide correct classifications. In addition, the Savitzky-Golay smoothing reduced the spectral noise, made emission peaks more defined, and increased model fit. The three methods evaluated for honey classification were able to separate the four classes: the k-NN (k=3) and SVM (ν=0.5, γ=10^{-6}) models provided 100% correct classification for the external validation set, and PLS-DA (9 LV) model provided 94% of correct classification (Table 1).

SVM and k-NN methods do not allow a visualization of the relationship between spectral variables and the class clusters. Thus, the PLS-DA method was used for such visualization and interpretation. The scores plot (Fig. 2) shows the separation of the four honey classes in the first three LVs. The PLS-DA model classified correctly all validation samples, except for a F sample, which was classified as region C honey.

The correlation between the spectral variables and the honey classes was assessed using loading and scores values. This analysis reveals that M samples were separated by the 1st LV (positive values), the CH samples by the 2nd LV (negative values), and the C and F samples were separated by the 3rd LV (C with negative

Table 1. Evaluation of Preprocessing Strategy for Each Classification Method

Preprocessing	Correct Classification					
	PLS-DA		k-NN		SVM	
	Cal	Val	Cal	Val	Cal	Val
MC	87%	46%	33%	57%	46%	45%
BC+MC	84%	46%	33%	57%	64%	53%
1st der+MC	91%	60%	32%	41%	28%	40%
2nd der+MC	87%	60%	29%	26%	36%	58%
Sm+MC	97%	78%	37%	46%	71%	64%
Sm+1st der+MC	94%	75%	42%	46%	50%	50%
Sm+2nd der+MC	91%	55%	37%	52%	36%	40%
MSC(mean)+MC	88%	28%	17%	31%	0%	25%
MSC(median)+MC	88%	52%	31%	33%	53%	36%
Norm.+MC	94%	47%	21%	37%	25%	25%
SNV+MC	88%	23%	17%	31%	17%	20%
GLSW+MC	100%	89%	100%	95%	100%	89%
Sm+GLSW+MC	100%	94%	100%	100%	100%	100%
EPO+MC	100%	59%	42%	56%	33%	35%
Pareto Scaling+MC	100%	88%	24%	36%	61%	62%
Poisson Scaling+MC	100%	69%	27%	31%	33%	40%
AS	100%	71%	37%	40%	64%	62%
BC+AS	100%	74%	32%	23%	0%	20%
1st der+AS	100%	69%	26%	41%	25%	45%
2nd der+AS	100%	74%	32%	51%	0%	15%
Sm+AS	100%	88%	29%	30%	54%	58%
Sm+1st der+AS	100%	69%	33%	51%	25%	50%
Sm+2nd der+AS	100%	69%	33%	46%	36%	45%
MSC(mean)+MC	100%	68%	14%	15%	0%	11%
MSC(median)+MC	100%	46%	17%	45%	0%	10%
Norm+AS	100%	56%	21%	31%	0%	20%
SNV+AS	100%	73%	17%	26%	28%	35%
GLSW+AS	100%	48%	100%	66%	100%	94%
Sm+GLSW+AS	100%	51%	100%	88%	100%	94%
EPO+AS	100%	74%	41%	50%	53%	43%

Note: Calibration set (Cal), external validation set (Val), mean centering (MC), baseline correction by Whittaker filter (BC), first derivative (1st der), second derivative (2nd der), smoothing (Sm), multiplicative scatter correction (MSC), normalization by area (Norm.), standard normal variate (SNV), generalized least squares weighting (GLSW), external parameter orthogonalization (EPO), and autoscaling (AS).

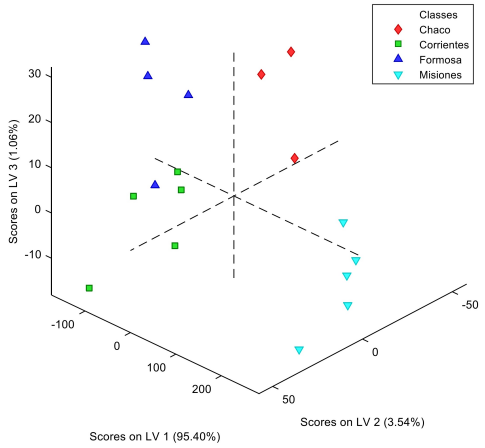

Fig. 2 Score plot of the PLS-DA model (only validation samples).

and F with positive values). The score plot also shows a greater separation of class M from the others, while classes C and F were more similar. These results corroborate the elemental composition of samples (Table 2), obtained by assigning spectral emission lines according to the NIST LIBS database.[41] A typical LIBS spectrum of a honey sample showing the emission lines that influenced class discrimination is shown in Fig. 3.

Class M samples had a relatively lower N content, while C and F samples showed the relatively higher content of this element, suggesting that C and F honeys have a high protein content in contrast to M honey. In addition, the C samples showed the relatively higher Ca content, resulting in the separation of this class by the 3rd LV of the model, and the medium K and Fe content provided the separation of the F samples. The CH samples were

Table 2. Emission Lines Related to Each Class

Class	Peak (nm)	NIST assignments	Intensity among classes
	499.5	N II (499.6 nm)	lowest
	552.9	N I (553.0 nm)	lowest
Misiones	553.5	N II (553.5 nm)	lowest
	567.6	N II (567.6 nm)	lowest
	568.5	N II (568.6 nm)	lowest
	324.7	Cu I (324.7 nm)	highest
Chaco	404.1	Mn I (404.1 nm)	medium
	434.7	Mn II (434.6 nm)	medium
	396.9	Ca II (396.9 nm)	highest
Corrientes	422.8	Ca I (422.7 nm)	highest
	466.2	N I (466.2 nm)	highest
	404.2	K I (404.4 nm)	medium
Formosa	439.7	Fe II (439.8 nm)	medium
	464.3	N II (464.3 nm)	highest

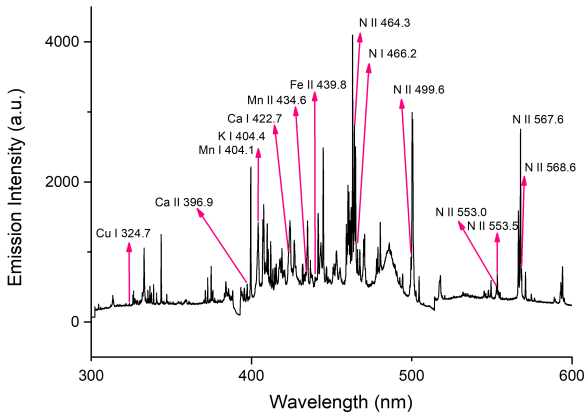

Fig. 3 Typical LIBS spectrum of a honey sample with emission line assignments related to the studied classes.

distinguished from the others by their relative higher levels of Cu and medium levels of Mn, and N did not show significant influence on segregation.

Three class of samples were separated according to the N content, suggesting that N plays a fundamental role in discriminating the geographical origin of honey. According to Imdorf *et al.*,[42] bees feed mainly on nectar and pollen, the latter being the main source of protein for the entire colony. Thus, the supply and quality of pollen, which directly influence the amount of N, could be related to the geographical production of honey. Furthermore, Fechner et al.[10] using ICP-MS data from the same samples used here, obtained a classification method for geographical origin reaching 76% of prediction accuracy. These results suggest that the absence of N in the data set may decrease the accuracy of the predictions. SD-LIBS presented attractive features for authentication of honey in terms of cost and performance, in addition to the ability to measure N, which is not feasible with ICP-MS. Thus, the methods developed provide new horizons for honey quality analysis.

CONCLUSIONS

Authentication of geographical origin of Argentine honey was assessed using a low-cost SD-LIBS and chemometric tools. Adequate spectral preprocessing provided k-NN and SVM models capable of accurately classifying honey according to their production regions. The results suggested N as the most important element to discriminate the studied classes. Complementary contributions from Ca, K, Cu, Fe, and Mn were also important for geographical discrimination of honey. Considering the possibility of measuring N and the importance of this element for geographical discrimination of honey samples, the proposed methods place LIBS in a prominent position in comparison with the conventional atomic techniques generally used for geographical analysis of honey (*e.g.* FAAS, ICP-OES and ICP-MS). Furthermore, the use of SD-LIBS provides fast, clean and direct analysis, providing a low-cost device for the control of food quality.

AUTHOR INFORMATION

Corresponding Author

* E.C. Ferreira

Email address: edilene.c.ferreira@unesp.br

Notes

The authors declare no competing financial interest.

ACKNOWLEDGMENTS

The authors would like to thank Asociación de Universidades Grupo Montevideo for exchange scholarship to D.C.F. and the Conselho Nacional de Desenvolvimento Científico e Tecnológico (CNPq) for the research grant to E.C.F. (308200/2018-7) and Fundação de Amparo à Pesquisa do Estado de São Paulo (FAPESP) grant number 2019/07537-6.

REFERENCES

1. C. European, Food Fraud, https://ec.europa.eu/food/safety/food-fraud_en (accessed 4 April 2019)
2. X. Zhou, M. P. Taylor, H. Salouros, and S. Prasad, *Sci. Rep.*, 2018, **8**, 1–11. https://doi.org/10.1038/s41598-018-32764-w
3. G. Cebrero, O. Sanhueza, M. Pezoa, M. E. Báez, J. Martínez,

M. Báez, and E. Fuentes, *Food Chem.*, 2020, **315**, 126296. https://doi.org/10.1016/j.foodchem.2020.126296

4. S. Đogo Mračević, M. Krstić, A. Lolić, and S. Ražić, *Microchem. J.*, 2020, **152**, 104420. https://doi.org/10.1016/j.microc.2019.104420
5. W. Von Der Ohe, L. Persano Oddo, M. L. Piana, M. Morlot, and P. Martin, *Apidologie*, 2004, **35**, S18–S25. https://doi.org/10.1051/apido:2004050
6. O. Anjos, C. Iglesias, F. Peres, J. Martínez, Á. García, and J. Taboada, *Food Chem.*, 2015, **175**, 128–136. https://doi.org/10.1016/j.foodchem.2014.11.121
7. M. V Baroni, N. S. Podio, R. G. Badini, M. Inga, H. A. Ostera, M. Cagnoni, E. A. Gautier, P. P. García, J. Hoogewerff, and D. A. Wunderlin, *J. Agric. Food Chem.*, 2015, **63**, 4638–4645. https://doi.org/10.1021/jf5060112
8. B. L. Batista, L. R. S. da Silva, B. A. Rocha, J. L. Rodrigues, A. A. Berretta-Silva, T. O. Bonates, V. S. D. Gomes, R. M. Barbosa, and F. Barbosa, *Food Res. Int.*, 2012, **49**, 209–215. https://doi.org/10.1016/j.foodres.2012.07.015
9. G. Di Bella, V. Lo Turco, A. G. Potortı, G. D. Bua, M. R. Fede, and G. Dugo, *J. Food Compos. Anal.*, 2015, **44**, 25–35. https://doi.org/10.1016/j.jfca.2015.05.003
10. D. C. Fechner, M. J. Hidalgo, J. D. Ruiz Díaz, R. A. Gil, and R. G. Pellerano, *Food Biosci.*, 2020, **33**, 483–490. https://doi.org/10.1016/j.fbio.2019.100483
11. J. C. R. García, R. I. Rodríguez, R. M. P. Crecente, J. B. García, S. G. Martín, and C. H. Latorre, *J. Agric. Food Chem.*, 2006, **54**, 7206–7212. https://doi.org/10.1021/jf060823t
12. H. Kaygusuz, F. Tezcan, F. Bedia Erim, O. Yildiz, H. Sahin, Z. Can, and S. Kolayli, *LWT - Food Sci. Technol.*, 2016, **68**, 273–279. https://doi.org/10.1016/j.lwt.2015.12.005
13. A. Terrab, D. Hernanz, and F. J. Heredia, *J. Agric. Food Chem.*, 2004, **52**, 3441–3445. https://doi.org/10.1021/jf035352e
14. I. K. Karabagias, A. P. Louppis, S. Karabournioti, S. Kontakos, C. Papastephanou, and M. G. Kontominas, *Food Chem.*, 2017, **217**, 445–455. https://doi.org/10.1016/j.foodchem.2016.08.124
15. H. Chen, C. Fan, Q. Chang, G. Pang, X. Hu, M. Lu, and W. Wang, *J. Agric. Food Chem.*, 2014, **62**, 2443–2448. https://doi.org/10.1021/jf405045q
16. Z. Vincevica-Gaile, M. Klavins, V. Rudovica, and A. Viksna, *WIT Trans. Ecol. Environ.*, 2011, **167**, 211–220. https://doi.org/10.2495/ST110191
17. S. Silici, O. D. Uluozlu, M. Tuzen, and M. Soylak, *J. Hazard. Mater.*, 2008, **156**, 612–618. https://doi.org/10.1016/j.jhazmat.2007.12.065
18. E. Yarsan, F. Karacal, I. G. Ibrahim, B. Dikmen, A. Koksal, and Y. K. Das, *Bull. Environ. Contam. Toxicol.*, 2007, **79**, 255–258. https://doi.org/10.1007/s00128-007-9034-9
19. C. Maione, F. Barbosa, and R. M. Barbosa, *Comput. Electron. Agric.*, 2019, **157**, 436–446. https://doi.org/10.1016/j.compag.2019.01.020
20. M. Oroian and S. Ropciuc, *Comput. Electron. Agric.*, 2019, **157**, 371–379. https://doi.org/10.1016/j.compag.2019.01.008
21. S. Ghanavati Nasab, M. Javaheran Yazd, F. Marini, R. Nescatelli, and A. Biancolillo, *Chemom. Intell. Lab. Syst.*, 2020, **202**, 104037. https://doi.org/10.1016/j.chemolab.2020.104037
22. D. P. Aykas, M.-L. Shotts, and L. E. Rodriguez-Saona, *Food Control*, 2020, **117**, 107346. https://doi.org/10.1016/j.foodcont.2020.107346
23. T. V. Silva, S. Z. Hubinger, J. A. Gomes Neto, D. M. B. P. Milori, E. J. Ferreira, and E. C. Ferreira, *Spectrochim. Acta Part B At. Spectrosc.*, 2017, **135**, 29–33. https://doi.org/10.1016/j.sab.2017.06.015
24. X. Li, S. Yang, R. Fan, X. Yu, and D. Chen, *Opt. Laser Technol.*, 2018, **102**, 233–239. https://doi.org/10.1016/j.optlastec.2018.01.028
25. B. A. Alfarraj, H. K. Sanghapi, C. R. Bhatt, F. Y. Yueh, and J. P. Singh, *Appl. Spectrosc.*, 2018, **72**, 89–101. https://doi.org/10.1177/0003702817733264
26. G. Bilge, H. M. Velioglu, B. Sezer, K. E. Eseller, and I. H. Boyaci, *Meat Sci.*, 2016, **119**, 118–122. https://doi.org/10.1016/j.meatsci.2016.04.035
27. M. C. Lázaro, C. P. Morais, T. V. Silva, G. S. Senesi, D. Santos Júnior, J. A. Gomes Neto, and E. C. Ferreira, *Anal. Letters*, Accepted. https://doi.org/10.1080/00032719.2020.1833021
28. Z. Zhao, L. Chen, F. Liu, F. Zhou, J. Peng, and M. Sun, *Sensor,* 2020, **20**, 1878. https://doi.org/10.3390/s20071878
29. A. Velásquez-Ferrín, D. V. Babos, C. Marina-Montes, and J. Anzano, *Appl. Spectrosc. Rev.*, 2020, 1–21. https://doi.org/10.1080/05704928.2020.1810060
30. Q. Zeng, F. Deng, Z. Zhu, Y. Tang, B. Wang, Y. Xiao, L. Xiong, H. Yu, L. Guo, and X. Li, *Plasma Sci. Technol.*, 2019, **21**, 034006. https://doi.org/10.1088/2058-6272/aadede
31. Q. Zeng, Z. Zhu, F. Deng, X. Zhu, B. Wang, Y. Xiao, L. Xiong, H. Yu, L. Guo, and X. Li, *Acta Photonica Sin.*, 2018, **47**, 847014. https://doi.org/10.3788/gzxb20184708.0847014
32. G. Nicolodelli, J. Cabral, C. R. Menegatti, B. Marangoni, and G. S. Senesi, *TrAC - Trends Anal. Chem.*, 2019, **115**, 70–82. https://doi.org/10.1016/j.trac.2019.03.032
33. A. L. Vieira, T. V. Silva, F. S. I. de Sousa, G. S. Senesi, D. S. Júnior, E. C. Ferreira, and J. A. G. Neto, *Microchem. J.*, 2018, **139**, 322–326. https://doi.org/10.1016/j.microc.2018.03.011
34. Y. W. Chu, S. S. Tang, S. X. Ma, Y. Y. Ma, Z. Q. Hao, Y. M. Guo, L. B. Guo, Y. F. Lu, and X. Y. Zeng, *Opt. Express*, 2018, **26**, 10119. https://doi.org/10.1364/OE.26.010119
35. M. Barker and W. Rayens, *J. Chemom.*, 2003, **17**, 166–173. https://doi.org/10.1002/cem.785
36. M. A. Sharaf, D. L. Illman, and B. R. Kowalski, *Chemometrics*, Wiley, New York, NY, 1986
37. C.-C. Chang and C.-J. Lin, *Neural Comput.*, 2001, **13**, 2119–2147. https://doi.org/10.1162/089976601750399335
38. R. I. Eigenvector, Eigenvector Research Documentation, http://wiki.eigenvector.com/index.php?title=Advanced_Preprocessing
39. J. A. Da-Col, W. F. C. Dantas, and R. J. Poppi, *Quim. Nova*, 2018, **41**, 345–354. http://dx.doi.org/10.21577/0100-4042.20170149
40. A. Savitzky and J.E.M. Golay, *Anal. Chem.*, 1964, **36**, 1627–1639. http://dx.doi.org/10.1021/ac60214a047
41. A. Kramida, K. Olsen, Y. Ralchenko, and Team, NIST LIBS Atomic Spectra Database Lines Form, https://physics.nist.gov/PhysRefData/ASD/lines_form.html
42. A. Imdorf, M. Rickli, V. Kilchenmann, S. Bogdanov, and H. Wille, *Apidologie*, 1998, **29**, 315–325. https://doi.org/10.1051/apido:19980402